analytical chemistry

Article

pubs.acs.org/ac

Development of Evaporative Light Scattering Detector for Capillary Electrochromatography and Capillary Liquid Chromatography

Wenli Zhou, Wenbin Kan, Yuhong Wang, Yuanyuan Liu, Yan Wang, and Chao Yan*

School of Pharmacy, Shanghai Jiao Tong University, Shanghai, P. R. China

Supporting Information

ABSTRACT: The paper describes a microfluidic evaporative light scattering detector (μELSD) for capillary electrochromatography and capillary liquid chromatography. The detector, consisting of a microfluidic nebulizer, a miniaturized evaporative module, a sheath gas module, and a light scattering chamber, was developed and optimized. Carrier gas exits from an extremely narrow circular gap (about 5 μm) between the spraying capillary o.d. and the nozzle i.d., impacting on the mobile phase liquid with supersonic velocity, to nebulize the effluent of a few hundred nL/min from the capillary outlet. The evaporation process was found to be accomplished at ambient temperature. A sheath gas module featuring a structural necking subsequent to drift tube endings was found to enhance the reproducibility and increase the S/N. Excellent linearity of the optimal μELSD was 3 orders of magnitude (0.2−40 ng; R^2 = 0.9998). The limit of detection (LOD) for glucose with a capillary column was 100 pg. Finally, the μELSD coupled to pressurized capillary eletrochromatography (pCEC) was applied to the analysis of six active components in traditional Chinese medicine extract, demonstrating the feasibility of the detector for capillary liquid separation system.

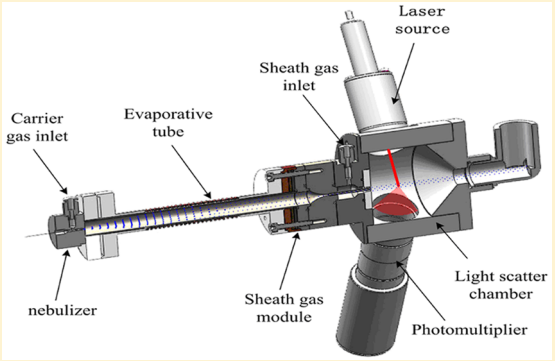

The evaporative light scattering detector (ELSD) is a universal detector for high-performance liquid chromatography (HPLC), which has also been adapted for detection in capillary electrophoresis.[1] ELSDs are capable of analyzing the substances, provided that their volatility is lower than that of the mobile phase. Moreover, they are suitable to detect compounds that have low light absorbance and are difficult to detect with ultraviolet (UV). Another benefit of ELSD vis-à-vis other universal detection methods (e.g., refractive index detector, RI) is that gradient mobile phases can be used without baseline drift.[2] The ELSD operates by nebulizing the column effluent into an aerosol or spray. The aerosol passes through a heated drift tube where the droplets evaporate, leaving behind solute particles. Afterward the solute particles pass through a light beam and scatter light. The scattered photons are detected by a photomultiplier and represent the amount of the solute in the column effluent.

Capillary separation system in the liquid phase is mainly represented by capillary liquid chromatography (CLC), capillary electrophoresis (CE), and capillary electrochromatography (CEC). Pressurized CEC (pCEC) is a typical capillary separation system, featuring a hybrid separation technique that combines CLC and CE and is capable of three modes of separations, i.e., CLC, CE, and pCEC.[3] With a packed or coated capillary column, it can be performed as a CLC when only high hydraulic pressure is used and as a pCEC when both pumps and high-voltage power supply are utilized.[4] With a capillary in which there are no packed or coated stationary phase but filled with buffer, CE can be implemented. Moreover, pCEC has additional advantages, such as high separation efficiency, high selectivity, quantitative sample injection with a rotary-type valve, and gradient elution similar to that in HPLC.[5]

Many types of detectors have been developed for the capillary liquid separation system, including UV, electrochemical (EC), laser-induced fluorescence (LIF), and mass spectrometer (MS).[6] Hitherto, a universal detector for capillary liquid separation system has been lacking. Interfacing of the capillary system with ELSD provides several advantages. First, a modicum of eluent in the capillary liquid separation system evaporates more easily than that of conventional HPLC, creating bulk liquids. Second, nebulization drops do not interact with flowing aerosol streams, thus band broadening of ELSD may be minimal.[7,8] However, a conventional ELSD which matches mL/min flow rate of the mobile phase in HPLC is not suitable for an effluent flow rate of nL/min to μL/min in a capillary separation system.

Hoffmann et al. developed an interface for the connection of packed microcolumn HPLC and a commercial ELSD.[9] Greibrokk also demonstrated an interface of microcolumn supercritical fluid chromatography (SFC) to ELSD.[10] A miniaturized ELSD for application with packed microcolumn HPLC or SFC was reported by Andersson et al.[11] They found that a makeup solvent (hexane at 30 μL/min) assisted in

Received: May 30, 2015
Accepted: August 16, 2015
Published: August 18, 2015

DOI: 10.1021/acs.analchem.5b02024
Anal. Chem. 2015, 87, 9329−9335

proper effluent nebulization, while the flow rate of the mobile phase was 5−100 μL/min, too great for CLC or pCEC. Recently, Gaudin et al. adapted a commercial detector to micro and CLC, based on the predicted size of the nebulized droplets via the Nukiyama and Tanasawa empirical equation.[12] Alexander et al. developed a miniaturized nozzle,[13] whereas the annular space between the spraying needle and the nebulization tube was 83 μm. While the above-mentioned authors were concerned seriously about nebulization modification, others were focused on the optimization of the evaporative system.[14]

The aim of this work is to develop a μELSD as a detector for a capillary liquid separation system and to comprehensively design its components including nebulization, evaporation, sheathing process, and light scattering chamber. Microfluidic nebulizer was designed and optimized to accommodate an effluent flow rate of 0.1 to 2 μL/min without makeup liquid. The dimension of a straight drift tube was optimized to 12 mm i.d. × 14 mm o.d. × 20 cm length that could accommodate the spray angle and evaporate at room temperature. A newly designed sheath gas module subsequent to drift tube ending was investigated that could enhance the reproducibility and increase the S/N. The fine linearity of the present μELSD ranged from 0.2 to 40 ng and the LOD with C_{18} capillary column was as low as 100 pg (n = 3). As to validate that the instrument can be used on capillary liquid separation system, pCEC coupled to μELSD was applied to the separation of platycodin D, peimisine, oleanolic acid, imperialine, peimine, and peiminine in traditional Chinese medicine extract, in which many components are lacking of conjugation groups in the molecular structures (shown in Figure S-1) and have no strong absorption in the region of ultraviolet and visible spectra.[15,16]

EXPERIMENTAL SECTION

Instrumentation. Like most conventional ELSDs, the newly designed μELSD includes four main parts, i.e., nebulization of the chromatography effluent, evaporation of the aerosol particles, light scattering by the aerosol, and detection of the scattered light.[17] While the liquid mobile phase flow rate in capillary separations is usually in the range of nL/min to μL/min, the nebulizer, drift tube and light scattering chamber are well developed and optimized.

The crux of the detector coupling to capillary separation system is converting the lower flow rate effluent into aerosol via nebulization. The μELSD still use a concentric pneumatic nebulizer (seeing Figure 1), which involves impacting the mobile phase with high velocity gas, creating high frictional forces over liquid surfaces and causing liquid disintegration into spray droplets.[18] The nebulizer was made up of a nozzle and spraying needle. The spraying needle was fused-silica capillary with 50 μm i.d./360 μm o.d. The capillary was axially fastened with PEEK tubing, which was connected to the nebulizer through a PEEK fitting. The end of the capillary was aligned to the nozzle end. The details of the nozzle outlet were shown as a cross-sectional view in Figure 1. The effluent flowed through the spraying capillary and the carrier gas was introduced from a connector and passed through the annular gap between the capillary o.d. and the nozzle i.d., which is noted as δ. A high relative velocity between the carrier gas, usually pure nitrogen or argon, and mobile phase are generated and expands to supersonic velocity that can cause fine droplets. It follows that when gas flow rate is constant, to achieve the supersonic condition, the annular gap should be extremely narrow. Then nebulization can be performed efficiently at a relatively low volumetric gas flow rate.[11] Likewise, the lower the mobile phase flow rate, the smaller must be the annular gap of the nebulizer nozzle to accommodate the low level flow rate of the mobile phase. It is reported that design and operation of the nebulizer significantly affect size distribution of resultant aerosols and thus instrument performance,[10,19] hereby the new design structurally concerns about decreasing the parameter δ. The annular gap of conventional ELSDs is usually 0.1 mm, whereas the nozzle i.d. was machined by microdrilling to 370−470 μm, and the inner wall was subsequently electro-polished as to avoid roughness influences on gas flow, thus the gap was narrowed down to about 5 μm.

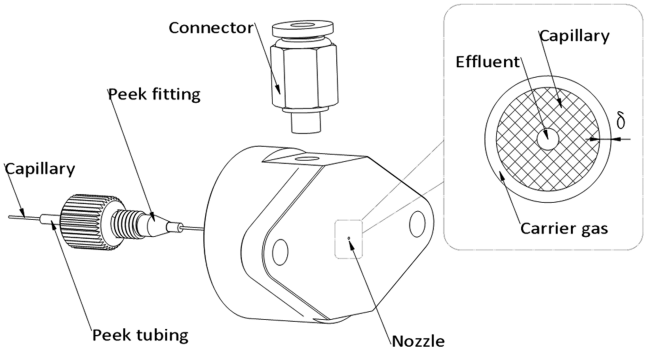

Figure 1. Detailed diagram of the microfluidic nebulizer.

The aerosol generated in the nebulization step is then driven by the carrier gas to the evaporative chamber, where the mobile phase evaporates to form analyte particles. In conventional ELSDs, the drift tube is usually in shape of a coil with 130 cm length × 1/2 in. or 1 in. in diameter. The optimized drift tube of this μELSD consisted of a stainless steel tube with only 20 cm length × 12 mm i.d. × 14 mm o.d. It was heated by heating coils wrapped around, and temperature can be controlled ranging from ambient temperature to 130 °C.

The main advantage of using sheath flow is that analytes exiting from the drift tube can be confined within the annular flow of gas, i.e., sheath gas, as they pass through the optics bench. This stabilized the flow trajectories in the optical bench and reduces noises.[19] Another advantage of sheath gas is that it prevents the carrier gas as well as the sample from impacting on the walls of optics bench.[20] As the flow rate of μELSD is in order of μL/min, much smaller than that of ELSDs, in order of mL/min, it follows that when the aerosol exits the evaporative chamber, very few analytes passes through the light beam, therefore sheath gas is necessary for the μELSD. Almost all sheath apparatus in prior art is a straight drift tube axially with a sheath sleeve. Herein the apparatus was improved via the structural necking subsequent to the drift tube ending as shown in Figure 2, regarding that the diameter of the analyte flow could match the center core of a focused laser beam and increase the probability of analytes detection. The drift tube was connected to sheath gas nozzle via heat insulator, which prevented overheat of solute analytes and influences on the photomultiplier (PMT) of later light scattering system. The structural necking was manufactured by electrical discharge machining, then its inner wall was electro-polished and had a fine surface finish. The stainless steel tube, dimensions by 5.0 mm i.d. × 6.0 mm o.d. × 2 cm length, was welded to the end of sheath gas nozzle as to further reduce the flow diameter. The

DOI: 10.1021/acs.analchem.5b02024
Anal. Chem. 2015, 87, 9329−9335

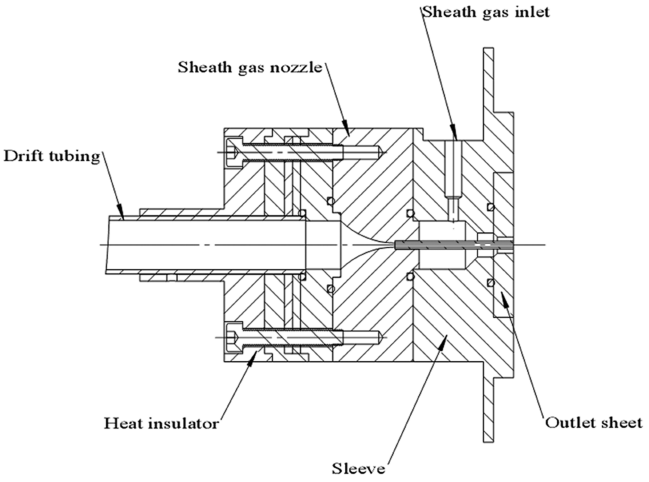

Figure 2. Part sectioned view of the sheath gas apparatus.

auxiliary gas was introduced into the sleeve from sheath gas inlet, and it formed the sheath gas where it passed through the circular orifice between the o.d. (6.0 mm) of the stainless steel tube and the i.d. (7.0 mm) of the hole in the outlet sheet.

The last step is light scattering detection in an optics bench. It commonly consists of light source, PMT, and two light traps (Figure 3). When analytes exit from drift tube and are impinged on by the laser beam, three light scattering regimes could occur, depending on the ratio of the particle diameter (D) and wavelength (λ) of the light source, i.e., Rayleigh scattering (occurring for particles where $D/\lambda < 0.1$), Mie scattering ($D/\lambda > 0.1$, but <10) and refraction-reflection ($D/\lambda > 10$).[12] The light scattered is detected at an angle of 120°. It was reported that in light scattering detection signal response is directly related to the light intensity, amplifying the source intensity results in a proportional, detrimental increase in noise.[21] Herein it was found that light intensity had no influences on S/N as it increased proportionally with both signal and noise. Therefore, the light source was selected as a polychromatic 650 nm laser diode at 20 mW. In the newly designed optics bench, stray light was concerned seriously. Stray light is light in an optical system, which was not intended in the design. The light may be from the intended source but follow paths other than intended.[22] For instance, stray light caused by a faint halo originating from the diode laser, and light reflection from the opposite direction to the laser source can significantly increase noises. The faint halo was blocked by a slit in front of the laser source. A light trap with sloping wedges was designed to minimize back-reflection. Also these methods were valid to decrease noises and thus increase S/N.

pCEC-μELSD Analysis. As to investigate the performance of the instrument, analysis was performed on the μELSD coupled to pCEC. The schematic diagram of pCEC coupled with μESLD was shown on Figure 3.

The TriSep-2100 pCEC system (Unimicro Technologies, Pleasanton, CA) consisted of two hydraulic pumps, a four-port split valve, a manually operated six-port injection valve equipped with a 1 μL external sample loop, a high voltage power supply ±30 kV. A reversed-phase capillary column (Global Chromatography, Suzhou, China) of 15 cm × 150 μm i.d. packed with 3 μm C_{18} particles was used. The total pump flow rate was 50 μL/min and was split in the four-port split valve after the injection valve at a ratio of 50:1 resulting in a flow rate of 1.0 μL/min and an injection volume of 20 nL into the capillary. The inlet of the column was connected to the four-port valve (cross), with a positive voltage applied. The column outlet was connected to the spraying capillary of μELSD by a micro Tee and grounded.

Experiments were performed by CLC using the isocratic eluention of methanol/water (1:5, v/v) in order to test the reliability of the μELSD. Glucose standards were dissolved in the water at concentrations from 2000 to 5 μg/mL. Six active components, platycodin D, peimisine, oleanolic acid, imperialine, peimine, and peiminine, were dissolved in the methanol/water (1:1, v/v) as standard mixtures at concentrations as follows: 2.66, 4.52, 3.16, 3.81, 3.87, and 3.42 mg mL^{-1}. The gradient elution system used for the separation of six active components by pCEC consisted of a mobile phase (A) acetonitrile and a mobile phase (B) 10 mM triethylamine (TEA)/formic acid (FA) in water (pH = 11.0). The gradient elution was performed as follows: The initial eluent was a mixture of 30% A and 70% B. After 5 min, the content of A in the eluent was linearly increased to 40%. Then the percentage of A was changed to 60% in 5.01 min, then, increased to 90% over 10 min, and finally held at 90%. Unless stated otherwise, the orifice between the 380 μm i.d. nozzle and the 50 μm i.d./360 μm o.d. capillary was ∼10 μm, and the drift tube of the μELSD was maintained at 40 °C and the optimum flow rate of the nebulizing gas was 0.40 L/min. Specific chromatographic conditions were listed in the figure captions. Chromatographic data were collected by a N2000 chromatographic working station (Zhejiang University Zhida Information Engineering, Hangzhou, Zhejiang, China).

Chemicals. HPLC grade acetonitrile (ACN) and methanol were purchased from TEDIA. Analytical grade triethylamine and formic acid were obtained from Sinopharm Chemical Reagent (Shanghai, China). The distilled water was purchased from Nestle (Shanghai, China) and used for preparation of the standards and the aqueous mobile phase. Analytical grade

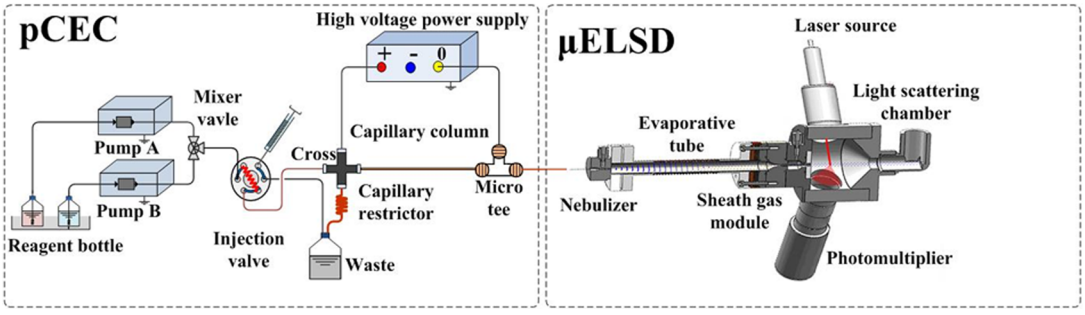

Figure 3. Schematic diagram of pCEC-μESLD.

DOI: 10.1021/acs.analchem.5b02024
Anal. Chem. 2015, 87, 9329−9335

glucose was purchased from Sinopharm Chemical Reagent (Shanghai, China). Platycodin D, peimisine, oleanolic acid, imperialine, peimine, and peiminine were purchased from Pure-one Bio Technology (Shanghai, China). The high-purity nitrogen was obtained from Shanghai Zongyuan Chemical (Shanghai, China) and utilized as the carrier gas. Prior to use, all mobile phases and sample solutions were filtered through a 0.22 μm membrane filter (Tianjin Hengao Technology Development, Tianjin, China) and sonicated for degassing.

RESULTS AND DISCUSSION

Nebulization Evaluation. The mean diameter of aerosol droplets significantly influences ELSD performance and actually an increase of the mean diameter results in response enhancement.[23] Mean diameter of aerosol droplets is characterized by D_{sv} (Sauter mean diameter), which can be estimated by the Nukiyama−Tanasawa empirical equation in the case of pneumatic nebulization.[15,24]

$$D_{sv} = \frac{0.585\sqrt{\sigma}}{(v_g - v_l)\sqrt{\rho}} + 53.22\left(\frac{\mu}{\sqrt{\sigma\rho}}\right)^{0.45}\left(\frac{Q_l}{Q_g}\right)^{1.5} \quad (1)$$

where σ is the surface tension (N/m), ρ is the density (kg/m^3), μ is the viscosity of the mobile phase (Pa s), $(v_g - v_l)$ is the relative velocity between the carrier gas and mobile phase, and Q_l/Q_g is the ratio of volumetric flow rates of mobile phase and that of the carrier gas.

From eq 1, it can be deduced that the decrease in the flow rate of the carrier gas with a constant or increased mobile phase flow rate results in an increase of D_{sv} and thus the enhancement of ELSD. While mobile phase could be incompletely nebulized and then induce excessive noises, if the flow rate of the carrier gas is too low. The D_{sv} was estimated by eq 1 under the nozzle i.d. was 370−470 μm, as shown in Table 1. The minimum orifice was narrowed down ∼5 μm. Thus, the instrument can be adapted for the 100 nL/min effluent flow rate (Table S-1 in the Supporting Information) and the optimal carrier gas flow rate for the 370 μm i.d. nozzle was lower to 0.25 L/min. The lower flow rate of carrier gas could decrease the sample dilution. As the orifice was narrowed down, the peak symmetry and the response of signal were improved (Figure S-2 in the Supporting Information). As the orifice was minimal, the pressure of the carrier gas reached a maximum. Given the instrument tolerance, the 380 μm i.d. nozzle and the 50 μm i.d./360 μm o.d. capillary was used in later experiments.

Table 1. Calculation of D_{sv} for the Micro-Fluidic Nebulizer with Glucose[a]

nebulizer i.d./capillary o.d. (μm)	δ (μm)	Q_g (L/min)	V_l (m/s)	V_g (m/s)	D_{sv} (μm)
470/360	55	2.00	8.5×10^{-3}	465	8.59
410/360	25	1.00	8.5×10^{-3}	551	7.24
380/360	10	0.40	8.5×10^{-3}	574	6.96
370/360	5	0.25	8.5×10^{-3}	727	5.50

[a] ρ = 1544 kg/m^3, σ = 71.97 × 10^{-3} N/m, and Q_l = 1.0 μL/min.

The microfluidic nebulization process was investigated by the CFD simulation which can promote the understanding of the atomizing process. The finite element model of the nozzle and the numerical results were described in the Supporting Information Figure S-3 (nebulizer i.d. = 380 μm, capillary o.d. = 360 μm, Q_g = 0.40 L/min). When the carrier gas expanded through the evaporative chamber, its velocity achieved supersonic conditions near the spraying tip.

Evaporation Investigation. The trajectory simulation as shown in the Supporting Information Figure S-3b implies that the diameter of the drift tube should be larger than the plume diameter as to avoid aerosol impact and accretion by tube. The results were validated experimentally for drift tube of small diameters (4.4 mm, 8.0 mm), causing much noises and decrease of the signal intensity (Figure S-4 in the Supporting Information). The optimal diameter of drift tube was 12 mm.

Figure 4 illustrated the response traces for 10 ng glucose at various evaporation temperatures with 0.5 L/min sheath gas and without sheath gas. It revealed that evaporation for μELSD could be accomplished at ambient temperature. The signal of glucose had no significant changes with the evaporation temperature decreasing from 120 to 25 °C. The noises was nearly constant with the temperature decreasing (∼20 μV), thus resulting in little decrease in S/N. This facilitated detection for volatile or thermally sensitive analytes.

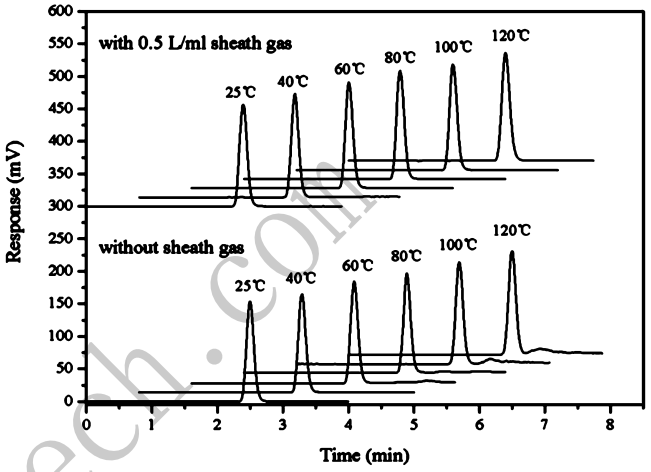

Figure 4. Response traces for 10 ng of glucose at various evaporation temperatures with (upper) and without (lower) sheath gas.

During the evaporative process, the droplets of mean diameter D_{sv}, become dry solute particles of diameter D_0, and light scattering depends on the size of the solute aerosols, which is given by

$$D_0 = D_{sv}\left(\frac{C}{\rho}\right)^{1/3} \quad (3)$$

From eq 3 and the calculated D_{sv} as shown in Table 1, the dry solute particles after evaporation can be evaluated, ∼488−936 nm, when C = 2 000 μg/mL. When the concentration of glucose was low (C = 5 μg/mL), the analytes diameter D_0 was estimated to range from 82 to 127 nm.

Evaporation occurs as a function of concentration, carrier gas flow rate, and temperature. High gas flow produces small droplets, requiring less heat to evaporate the solvent. Conversely, low gas flow produces large droplets, requiring more heat to evaporate the solvent. It was reported that the mechanisms for light scattering transfer from the Mie scattering regime, where particle diameters ranges in the order of hundreds of nanometers, to Rayleigh scattering regime with diameters below 100 nm.[25] From the calculation above, it is obvious that the scattering mechanism of the instrument was predominant in Mie scattering regime.

DOI: 10.1021/acs.analchem.5b02024
Anal. Chem. 2015, 87, 9329−9335

The calculation was ideally valid under the assumption that dry analytes were neither incompletely evaporated nor overheated. Nevertheless, it can be found in Figure 4 that ghost peaks occurred with the temperature increasing (without sheath flow). Since high temperature leads to a liquid viscosity decrease and Reynolds number increases, causes intensifying turbulence, and induces ghost peaks. The ghost peak in Figure 4 (lower) was caused by turbulence since it was found to disappear with the later-discussed sheath gas introduced.

Response to Sheath Flow. Figure 5 illustrated the S/N of 10 ng of glucose as a function of sheath flow rate. The S/N

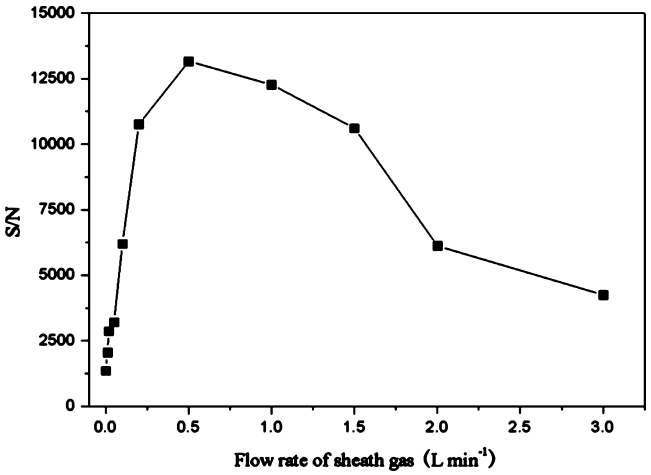

Figure 5. S/N of 10 ng glucose versus flow rate of sheath gas.

value increased with the increment of sheath gas flow, and the maximum occurred higher than 13 000 with the sheath gas at 0.5 L/min. Then S/N decreased with sheath gas increasing greater than 0.5 L/min. This phenomenon reveals that there exists an optimum of sheath gas flow rate to increase the S/N and thus decrease the limit of detection.

The comparison of six replicate injections of 10 ng glucose without and with 0.5 L/min sheath gas was shown in Table 2.

Table 2. Six Replicate Injections of 10 ng of Glucose

sequence	peak area[a] (mV s)	peak area[b] (mV s)
1	987	1084
2	954	1071
3	911	1080
4	942	1063
5	932	1065
6	983	1077
RSD	3.11%	0.78%

[a]Without sheath gas. [b]With 0.5 L/min sheath gas.

The RSDs of the peak area without and with sheath are 3.11% and 0.78%, respectively. It reveals that sheath gas can enhance the reproducibility of the instrument and be necessary for the μELSD. Furthermore, the peak area with sheath was greater than that without sheath as more analytes were reasonably concentrated to be scattered.

Evaluation of μELSD. The response for ELSDs has been commonly described as nonlinear and considered to follow the equation:[12]

$$A = am^b \quad (4)$$

where A is the peak area, m the injected amount, and a and b are numerical coefficients. The linear range of the present system was from 0.2 to 40 ng (R^2 = 0.9998; Figure S-5 in the Supporting Information). The lowest level of glucose that could reasonably be detected with the C_{18} capillary column was 100 pg (Figure 6).

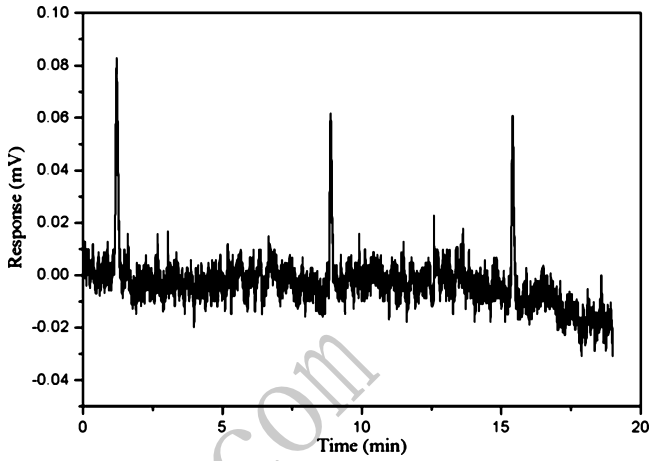

Figure 6. Three replicate injections of 100 pg glucose.

Application to Sample Analysis. The separation and determination were carried out by using a mixture of platycodin D, peimisine, oleanolic acid, imperialine, peimine, and peiminine as an example of analytical application. The analytes were difficult to be detected by UV−vis without any derivatization. The pK_a values of platycodin D, peimisine, oleanolic acid, imperialine, peimine, and peiminine were, respectively, estimated by software (Sci Finder) as 12.76 ± 0.7, 14.89 ± 0.7, 4.64 ± 0.7, 14.56 ± 0.7, 14.6 ± 0.7, 14.56 ± 0.7. Figure 7 showed the effects of the applied voltage on separation of the mixture. Under the pH value of 11.0, the oleanolic acid was negatively charged and fritillaria alkaloids (peimisine, imperialine, peimine, and peiminine) positively charged and platycodin D uncharged. The electrophoretic mobility of the oleanolic acid in the column was in the opposite direction to the pressurized flow and EOF. The electrophoretic mobility of the fritillaria alkaloids were in the same direction as EOF. The separation speed and resolution for the mixture were much better due to the difference in their electrophoretic mobility. In Figure 7, the separation of six active components was improved by changing the applied voltage, and the total analysis time of six active components was shortened from 15 min to less than 10 min. The resolutions of peak pairs 2 and 3 and 4 and 5 were calculated, and the results were listed in Table S-2.

Under the optimal conditions, the mass LODs (S/N = 3) for six active components were in the picogram range, shown in Supporting Information Table S-2. The precision, repeatability, and stability indicated a good reproducibility for the determination. It demonstrates that the feasibility of the μELSD coupled to capillary liquid separation system such as pCEC, CLC, and CE.

CONCLUSIONS

A microfluidic evaporative light scattering detector (μELSD) for CLC and pCEC was developed. The microfluidic nebulizer, miniaturized evaporative module, sheath gas module, and light

DOI: 10.1021/acs.analchem.5b02024
Anal. Chem. 2015, 87, 9329−9335

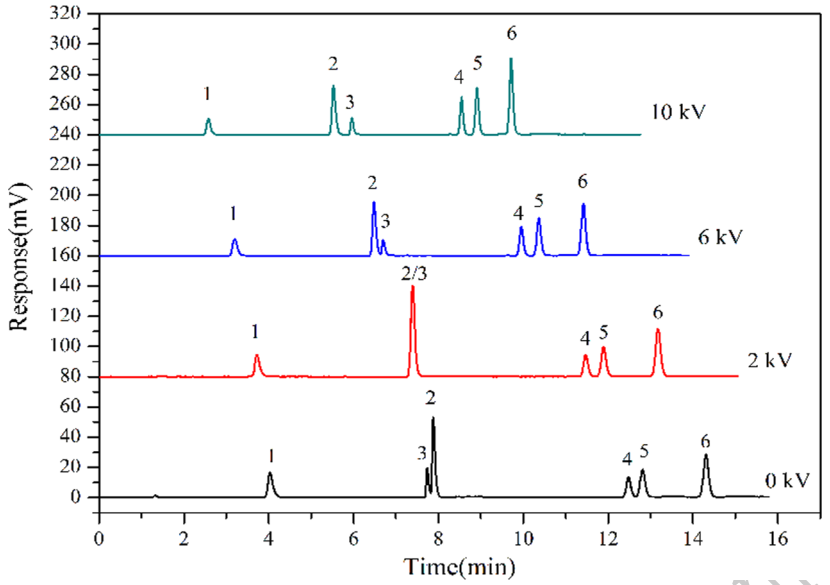

Figure 7. Electrochromatograms of six active components by pCEC-μELSD. Conditions: capillary column, 150 μm i.d. × 15 cm length, packed with 3 μm C_{18} particles; mobile phase, A = acetonitrile, B = 10 mM TEA/FA in water (pH = 11.0), 0−5 min, A from 30% to 40%; 5.01−10 min, A from 60% to 90%; finally held at 90% A; mobile phase flow rate, 1.0 μL/min; nebulizer, 380 μm i.d. nozzle with 50 μm i.d. × 360 μm o.d. spraying capillary; drift tube temperature, 40 °C; nebulizing gas flow, 0.40 L/min. Peaks: 1, platycodin D; 2, peimisine; 3, oleanolic acid; 4, imperialine; 5, peimine; 6, peiminine.

scattering chamber were comprehensively studied and optimized. The μELSD coupled to pCEC was applied to the separation of six active components, demonstrating the good separation of pCEC and the universality of μELSD. The analyses of complicated samples (the nonultraviolet and weakly ultraviolet active ingredients of traditional Chinese medicine, such as saponins, alkaloids, terpenoids, steroids, and so on as well as sugars, natural drugs, carbohydrates, amino acids, lipid compounds, polymers, etc.) will be more suitable and efficiently carried out by pCEC-μELSD.

■ ASSOCIATED CONTENT

Supporting Information

The Supporting Information is available free of charge on the ACS Publications website at DOI: 10.1021/acs.analchem.5b02024.

Additional experimental data and results (PDF)

■ AUTHOR INFORMATION

Corresponding Author

*E-mail: chaoyan@sjtu.edu.cn. Phone: +86-021-3420-5673. Fax: +86-021-3420-5908.

Author Contributions

The manuscript was written with the equal contribution of Wenli Zhou and Wenbin Kan. All authors have given approval to the final version of the manuscript.

Notes

The authors declare no competing financial interest.

■ ACKNOWLEDGMENTS

This research was financially supported by the National Key Scientific Instrument and Equipment Development Project (China), Grant Numbers 2011YQ150072 and 2011YQ15007202, and by the Science and Technology Support Plan of Suzhou (China), Grant Number SG201214.

■ REFERENCES

(1) Bouri, M.; Salghi, R.; Zougagh, M.; Rios, A. *Anal. Chem.* **2013**, *85*, 4858−4862.
(2) Strode, J. T. B.; Taylor, L. T. *J. Chromatogr. Sci.* **1996**, *34*, 261−271.
(3) Dittmann, M. M.; Rozing, G. P. *J. Chromatogr. A* **1996**, *744*, 63−74.
(4) Yan, C.; Schaufelberger, D.; Erni, F. *J. Chromatogr. A* **1994**, *670*, 15−23.
(5) Wu, Q.; Yu, X.; Wang, Y.; Gu, X.; Ma, X.; Lv, W.; Chen, Z.; Yan, C. *Electrophoresis* **2014**, *35*, 2470−2478.
(6) Yan, C. *Contemporary Microscale Separation Technology*; HNB Publishing: New York, 2013.
(7) Stolyhwo, A.; Colin, H.; Guiochon, G. *Anal. Chem.* **1985**, *57*, 1342−1354.
(8) Tarr, M. A.; Zhu, G.; Browner, R. F. *Appl. Spectrosc.* **1991**, *45*, 1424−1432.
(9) Hoffmann, S.; Norli, H. R.; Greibrokk, T. *J. High Resolut. Chromatogr.* **1989**, *12*, 260−264.
(10) Demirbuker, M.; Anderson, P.; Blomberg, L. *J. Microcolumn Sep.* **1993**, *5*, 141−147.
(11) Andersson, M. B.; Blomberg, L. G. *J. Microcolumn Sep.* **1998**, *10*, 249−254.
(12) Gaudin, K.; Baillet, A.; Chaminade, P. *J. Chromatogr. A* **2004**, *1051*, 43−51.
(13) Alexander, J. N. *J. Microcolumn Sep.* **1998**, *10*, 491−502.
(14) Guillarme, D.; Rudaz, S.; Schelling, C.; Dreux, M.; Veuthey, J. L. *J. Chromatogr. A* **2008**, *1192*, 103−112.
(15) Li, S. L.; Lin, G.; Chan, S. W.; Li, P. *J. Chromatogr. A* **2001**, *909*, 207−214.
(16) Dong, L. Y.; Zhang, Y. H.; Guo, T. T.; Liu, Y. J.; Qi, X.; Hou, Y. Y. *Chin. Pharm. J.* **2012**, *47*, 830−833.
(17) Ryan, D. C.; Yong, L. In *Advances in Chromatography*, Vol. *52*; CRC Press: Boca Raton, FL, 2014; pp 1−54.
(18) Hede, P. D.; Bach, P.; Jensen, A. D. *Chem. Eng. Sci.* **2008**, *63*, 3821−3842.
(19) Watson, J. T.; Sparkman, O. D. In *Introduction to Mass Spectrometry: Instrumentation, Applications and Strategies for Data Interpretation*, 4th ed.; John Wiley & Sons, Ltd.: Chichester, U.K., 2008; pp 639−688.

DOI: 10.1021/acs.analchem.5b02024
Anal. Chem. 2015, 87, 9329−9335

(20) Keller, R. A.; Nogar, N. S. *Appl. Opt.* **1984**, *23*, 2146−2151.
(21) Lucena, R.; Cárdenas, S.; Valcárcel, M. *Anal. Bioanal. Chem.* **2007**, *388*, 1663−1672.
(22) Sims, J. L. *Chromatographia* **2001**, *53*, 401−404.
(23) Megoulas, N. C.; Koupparis, M. A. *Crit. Rev. Anal. Chem.* **2005**, *35*, 301−316.
(24) Van der Meeren, P.; Vanderdeelen, J.; Baert, L. *Anal. Chem.* **1992**, *64*, 1056−1062.
(25) Dixon, R. W.; Peterson, D. S. *Anal. Chem.* **2002**, *74*, 2930−2937.

DOI: 10.1021/acs.analchem.5b02024
Anal. Chem. 2015, 87, 9329−9335